Investigating the Performance Enhancement of Copper Fins on Trapezoidal Thermochemical Reactor

Xiaojing Han, Shuli Liu, Liu Yang, Cheng Zeng, Ashish Shukla and Yongliang Shen

Original citation & hyperlink:
Han, Xiaojing, et al. "Investigating the performance enhancement of copper fins on trapezoidal thermochemical reactor." *Renewable Energy* (2019).
https://dx.doi.org/10.1016/j.renene.2019.11.052

ISSN 0960-1481

Publisher: Elsevier

Journal Pre-proof

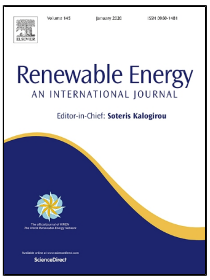

Investigating the Performance Enhancement of Copper Fins on Trapezoidal Thermochemical Reactor

Xiaojing Han, Shuli Liu, Cheng Zeng, Liu Yang, Ashish Shukla, Yongliang Shen

PII:	S0960-1481(19)31739-2
DOI:	https://doi.org/10.1016/j.renene.2019.11.052
Reference:	RENE 12600
To appear in:	*Renewable Energy*
Received Date:	13 June 2019
Accepted Date:	12 November 2019

Please cite this article as: Xiaojing Han, Shuli Liu, Cheng Zeng, Liu Yang, Ashish Shukla, Yongliang Shen, Investigating the Performance Enhancement of Copper Fins on Trapezoidal Thermochemical Reactor, *Renewable Energy* (2019), https://doi.org/10.1016/j.renene.2019.11.052

Investigating the Performance Enhancement of Copper Fins on Trapezoidal Thermochemical Reactor

Xiaojing Han[1], Shuli Liu[1,2,*], Cheng Zeng[2], Liu Yang[1], Ashish Shukla[2], Yongliang Shen[1]

[1] School of Mechanical Engineering, Beijing Institute of Technology, Beijing 100081, China

[2] School of Energy, Construction and Environment, Coventry University, Coventry, CV1 2HF, United Kingdom

*Corresponding Author at: School of Energy, Construction and Environment, Coventry University, Coventry CV1 2FB, UK. Email: Shuli.Liu@coventry.ac.uk

Abstract

Thermochemical energy storage has a great potential in thermal energy storage attracting extensive attention in building's applications. However, performance issues of the thermochemical reactor should be tackled to improve the overall performance. To enhance the heat transfer within the reactor, this study proposes a thermochemical reactor integrated with copper fins. The reactor features both heated air and water output in a discharging process. Using Zeolite 13X as the thermochemical material, experimental tests have been conducted and presented in this paper to investigate the performance of the reactor. According to the experiment, the copper fins reactor achieves better performance in both charging and discharging compared with the reactor without fins. In charging, copper fins reactor reduces charging time by 0.75 hours for the outlet air temperature reaching to the comparable level of the reactor without fins at 156.2 ℃. In discharging, the copper fins reactor achieves the peak outlet air temperature at 54.6 ℃ and the peak outlet water temperature at 39.4 ℃. Additionally, the reactor achieves energy storage density at 233 kWh/m^3 for material level and 128 kWh/m^3 for the reactor level. This paper provides valuable information for improving the reactor performance to achieve an optimal performance of a thermochemical energy storage system.

Keywords: Thermochemical reactor; Zeolite 13X/water; Copper fins; Reactor performance

Nomenclature

c_p	Specific heat at constant pressure, J/(kg·℃)	Subscripts	
$\dot{Q}$	Thermal power, kW	dis	discharging
Q	Energy, kWh	char	charging
$\dot{m}$	Mass flow rate of air, kg/s	in	inlet
RH	Relative humidity, %	out	outlet
t	Time, s		
T	Temperature,℃		
ω	Absolute humidity, g/kg		

1. Introduction

Currently, to tackle the energy consumption in buildings, especially in space heating and domestic hot water production, renewable energy technologies have been applied in buildings sector [1]. To improve the share of renewable energy in building's energy consumption, a promising way is to use thermal energy storage technologies.

Within the context, thermochemical energy storage stands out in the excellent characteristics including high energy storage density and low heat loss over sensible and latent energy storage technologies. For the application of space heating, it can store solar thermal energy in sunny days and release the heat during cloudy days or at night, increasing the share of solar energy in buildings [2].

As the principle of thermochemical energy storage, heat is stored in thermochemical materials in the form of chemical potential. Endothermic and exothermic reactions take place to store (charging process) and release energy (discharging process). The space where the charging and discharging processes take place is thermochemical reactor. Currently, the thermochemical reactor has been one of the major focuses in the research and development of a thermochemical energy storage system in building's applications.

1.1. The state-of-the-art of thermochemical reactor in building's applications

Tatsidjodoung et al. [3] have developed an open reactor with 80 kg zeolite as the thermochemical material, as shown in **Fig. 1**. The reactor is divided into 2 sub segments with 40 kg zeolite each. The two reactors enable parallel or serial connections. According to the experimental tests, in a discharging test, the temperature lift of 38 ℃ could be reached and in correlation to the inlet air humidity during continuous 8 hours discharging process. However, high pressure loss has been highlighted which increases electricity consumption of the system.

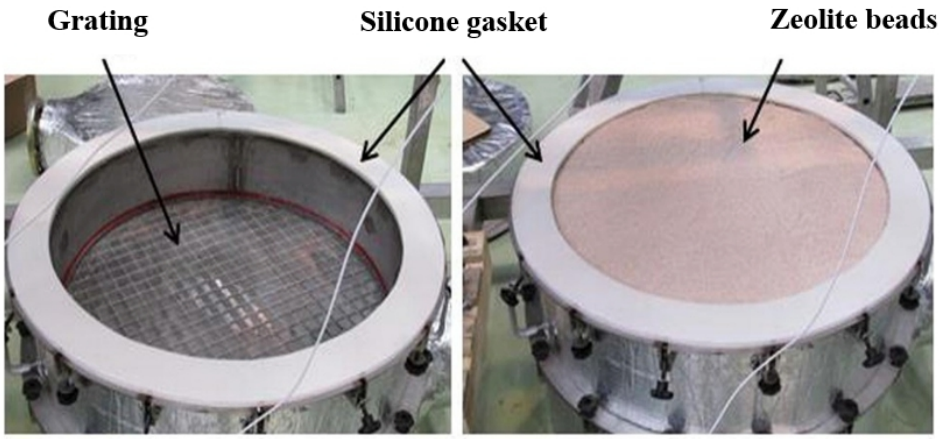

Fig. 1. Pictures of a zeolite vessel with grating support [3]

Recently, a system consists of four reactors has been reported by Gaeini et al [4], as shown Fig. 2. In this study, the experimental results show that the average energy density of 198 kWh/m^3 and 108 kWh/m^3 are obtained for thermochemical material and reactor, respectively. With one reactor containing 42.5 kg zeolite 13X, it can store 17 kWh energy for 7 hours and release 70% during a discharging process. According to the experimental statistics, however, relatively low power output has been presented due to the reactor structures.

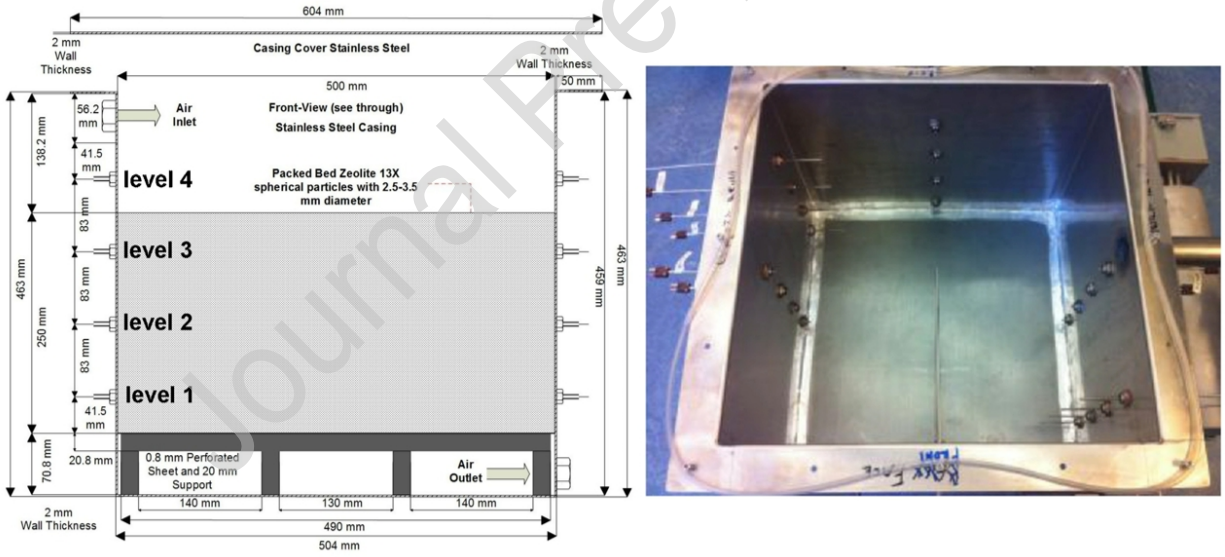

(a) side view (b) top view

Fig. 2. Pictures of reactor: (a) side view and (b) top view [4]

Additionally, the authors have investigated the feasibility for domestic hot tap water production [5]. The reactor is connected to an air-to-water heat exchanger where the released energy from the reactor is transferred to the water. According the experimental tests, energy densities for material and reactor are 112 kWh/m^3 and 61 kWh/m^3 respectively. The authors have reported that around 75% to 80% of the released energy can be stored in a water tank with water temperature up to 75 ºC.

For the same reactor, Alebeek et al. [6] also have investigated a household-scale open sorption

energy storage system with zeolite 13X/water working pairs. A maximum power of 4.4 kW and stored thermal energy of 54 kWh have been obtained in this system. They have reported that uneven distribution of flow through the bed reactor which has affected the reactor performance.

Zettl et al. [7] have investigated a moving material bed with 50 kg zeolite to provide space heating and hot water supply in domestic buildings, as shown in **Fig. 3**. According to the authors, the reactor can achieve a maximum thermal power of 1.5 kW adsorption heat up to 12 kWh. The rotation design has shown high specific thermal power, good controllability, low pressure drop inside the reaction bed. However, due to poor mechanical strength of zeolite, the issues are particles breakage and poor cycle stability after long time cycles.

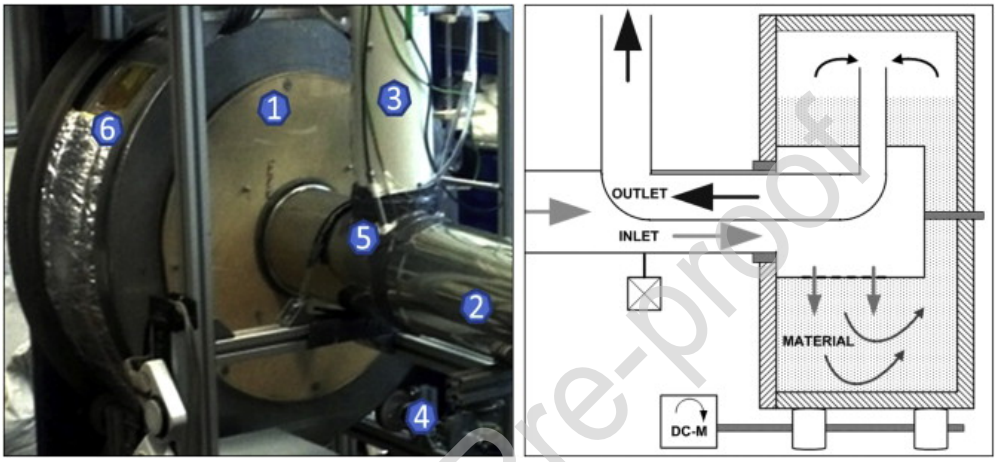

Fig. 3. Rotational drum reactor in buildings [7]

Christian et al. [8] have built a 41 kg zeolite thermochemical heat storage module to supply space heating at the temperature of 40 ℃ for residential buildings. The design is originated from a lab tests as shown in Fig. 4 (a), where zeolite spheres are integrated with a finned heat exchanger which is placed in a cylindrical vessel [9]. Water vapor is supplied to the vessel and water flows through the heat exchanger to extract heat in discharging. For the designed 3 kWh system, as shown in **Fig. 4** (b), experimental results have shown that zeolite temperature lift 31.2 ℃ under the adsorption temperature at 20 ℃ and evaporation temperature at 15 ℃. The maximum power of 971 W can be reached under desorption temperature at 103 ℃ and condensation temperature at 20 ℃, thus achieving a maximum specific power of 24 W/kg. However, the maximum material energy density of 83.4 kWh/m^3 and system energy density of 22.24 kWh/m^3 have been found in this experiment system. The relatively low energy density calls for optimization in the reactor structure and charging and discharging avenues.

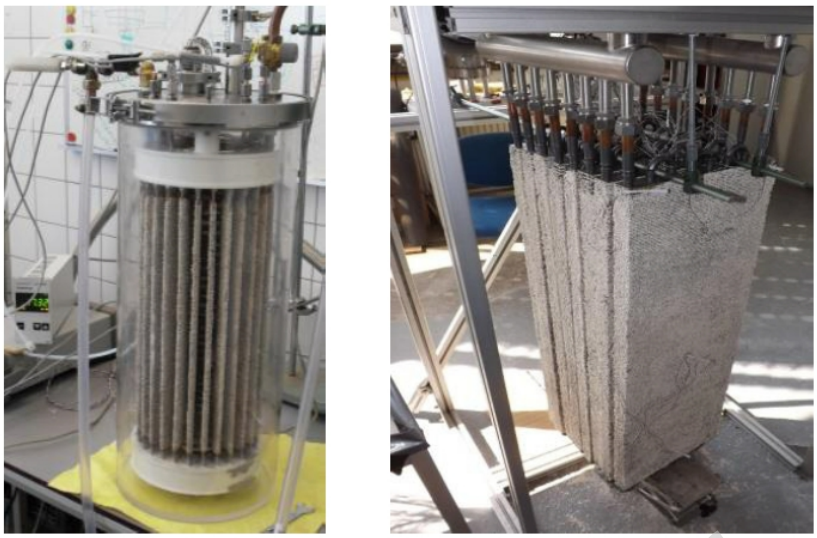

(a) (b)

Fig. 4. (a) Zeolite spheres attached on finned heat exchanger [9], (b) developed 3 kWh module in experimental test [8]

A number of studies have reported reactors for thermochemical energy storage as applied in buildings. However, further research and development is required to achieve a better reactor performance including: heat and mass transfer enhancement within reactor, high pressure drop of air flow across the reactor, heat extraction in discharging as applied in buildings, and thermal losses in charging and discharging cycles.

1.2. Aim, objectives and contributions of the paper

This study experimentally investigates heat transfer enhancement and the performance of a novel thermochemical reactor with copper fins. Zeolite 13X has been selected as thermochemical storage material due to it relatively high storage density and fast kinetic reaction, as demonstrated in Section 2. Section 3 demonstrates the experimental rig and details in the experimental tests. Heat and mass transfer of the reactor are improved by integrating with copper fins. Section 4 provides the experimental results and discussions about the reactor performance in charging and discharging. Conclusions and future work are given on Section 5. According to experimental tests, the integration of copper fins supports the reactor achieve an improved performance in both charging and discharging processes. In charging, under the experiment, the time consumption to reach a stable outlet air temperature has been reduced from 3.63 hours to 2.88 hours. In discharging, the fin pipes reactor has achieved a relatively higher peak outlet air temperature and peak outlet water temperature at 54.6 ℃ and 39.4 ℃, respectively. The paper contributes to the literature by providing insightful and valuable outputs for further improving the reactor performance with novel design and operational parameters optimization.

2. Thermochemical material selection

This section demonstrates the selection of the thermochemical materials considering advantages and disadvantages of hygroscopic salts and adsorbent materials.

2.1. Hygroscopic salts

Extensive research on salt hydrates is being carried out for thermal storage purposes, such as $MgCl_2$ [10], $MgSO_4$ [11, 12], LiCl [13, 14] and $SrBr_2$ [15, 16]. However, the studies have highlighted issues including solution carryover, mass transfer obstacles, swelling and agglomeration [17].

The hydrothermal stability issues are the change of crystal structure in hydration/dehydration, which reduce heat and mass transfer efficiency of the thermochemical reactor [18]. Specifically, the phenomenon of hard crust aggregation, deliquescence, and pulverization have been reported in the studies of $MgCl_2$, $MgSO_4$ [19], $CaCl_2$ [20], and $SrBr_2$ [21, 22]. Ferchaud [23] has reported slow reaction rates of $MgSO_4 \cdot 7H_2O$ under the a moist air flow of 100ml/min and water vapor pressure of 13 mbar operating conditions. $SrBr_2$ has been studied in thermochemical energy storage, particularly reacting from the hexahydrate to the monohydrate [24]. Michel et al. [25] reported it has the potential for continuous dehydration/hydration cycles. However, the high cost makes this material less attractive for large-scale storage applications [26]. $MgCl_2$ produces HCl gas in hydration and dehydration cycles, including temperature below 100 ℃ [23] and above 140 ℃ [27], which causes corrosion and safety concerns [28]. The deliquescence and overhydration below 40℃ easily occur, with limited thermochemical storage application.

2.2. Adsorbent materials

Adsorbent materials such as zeolite, silica gel, activated carbon have been showing advantages in thermochemical energy storage. They are more hydrothermally stable. Zeolites are hydrophilic sorbents with electrostatic charged framework and extra-framework cations [29]. The strong interaction between the electrostatic charged frameworks and water molecules ensures its water sorption capacity.

Artificially synthesized zeolites show higher bulk specific weight and better heat transfer performance than natural zeolites, mainly applying them in dehumidification cooling system, adsorption refrigeration and heat storage system [30]. Different types of zeolites have been developed for thermochemical energy storage applications, such as types 4A, 5A, 10X, 13X and Y. Zeolite 13X has been employed as adsorbent due to its high adsorption performance, good stability, relatively high energy storage density and low cost. It is non-toxic and non-flammable.

3. Description of the experimental rig

This section illustrates the experimental test rig of the copper fins reactor including the experiment system, reactor design, instrumentations, performance analysis indicator, and uncertainty analysis.

3.1. Facilities in the experimental rig

A thermochemical energy storage system has been built at the Beijing Institute of Technology, Beijing China, as shown in **Fig. 5**. The experimental rig includes fan, humidifier, air to air heat exchanger, electric heater, reactor, water tank, water pump and instrumentations. The fan drives ambient air through the reactor. An electric heater and ultrasonic humidifier provide heat and moisture of air to the reactor. Water flow is integrated in the reactor, driven by the water pump. Additionally, to reduce thermal losses, the whole system is insulated with 50 mm thick glass wool. Temperature, pressure, humidity and air velocity sensors, distributed in the inlet and outlet of reactor. Table 1 gives details of the key instrumentations.

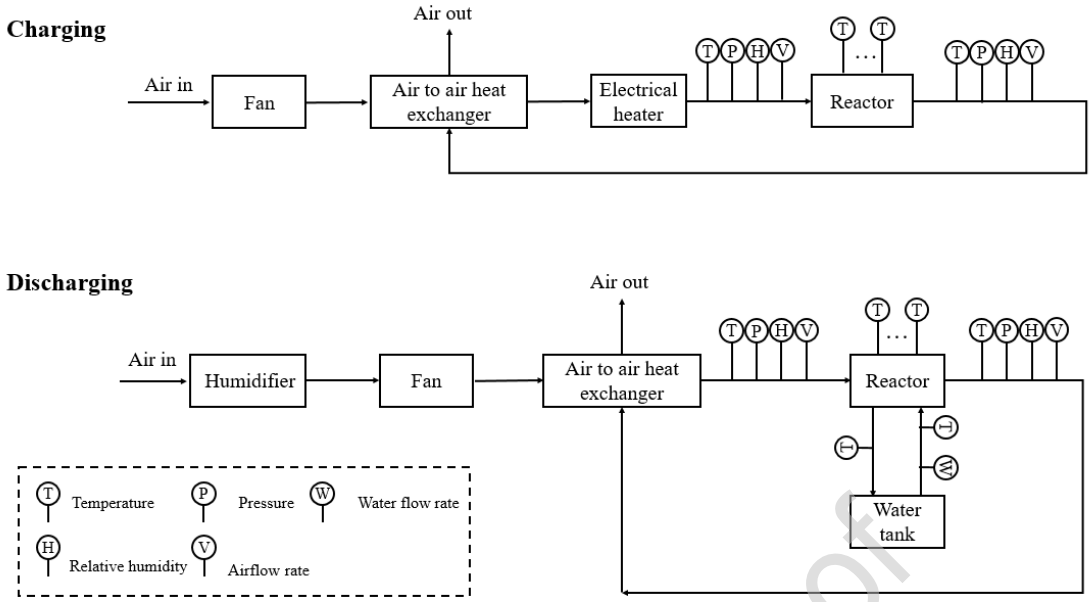

Fig. 5. The schematic diagram of charging/discharging cycles

Table 1

The details on the key instruments

Instruments	Specification	Quantity
Fan	Air volume: 2000 m^3/h, Pressure: 2000 Pa, Power: 15 kW	1
Ultrasonic humidifier	DRS-06A, Humidification capacity: 6 kg/hour, Power: 600 W	1
Plate heat exchanger	Type:ERA-500-500-360-5S Size: 500(L)*500(W)*360(H), Plate distance: 5 mm Exchange form: cross flow	1
Electric heater	Power: 15 kW	1
Water tank	Size: 500*500*900 mm^3	1
Water pump	Type:WD-016,Maximum flow rate:10 L/min, Power:0.12 kW, Frequency:50 Hz	1
Data logger	Type: TPC1061Ti, Input:24V DC/300mA	1
Sensors	Airflow rate: Range :0-100 m/s, Accuracy: 3%	2
	Reactor/air/water temperature: Range : -200-500℃, Accuracy: 3%	31
	Air humidity: Range : 0-100 %, Accuracy: 3%	2
	Air pressure: Range : 0-1000 Pa, Accuracy: 1%	2

Fig. 6 shows methodology of this study which demonstrates the experimental operating conditions, data measurements and calculations, and performance indicator. The study has conducted charging and discharging tests on 2 cases, smooth pipes and copper fins reactor. Smooth pipes reactor in case 1 is the reactor with no fin integration and copper fins reactor in case 2 has been integrated with fins on the water pipe. In discharging, the water pump is set to achieve water flow rate at 0.08 m^3/h.

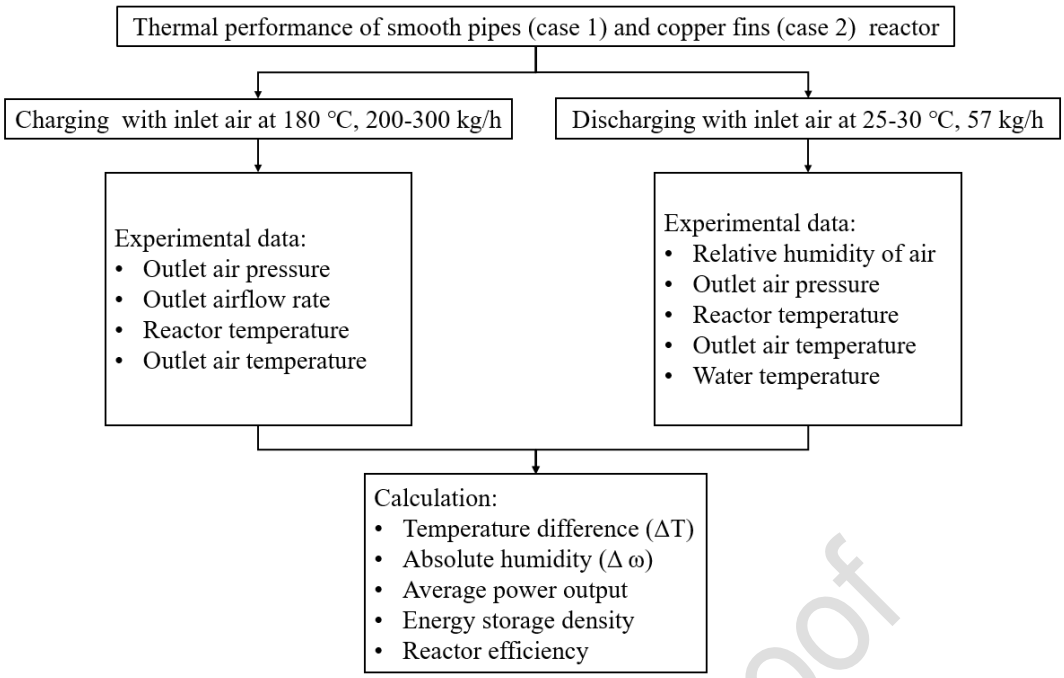

Fig. 6. Methodology of the study in graphic flow chart

3.2. Description of the copper fins thermochemical reactor

The reactor is in trapezoidal shape with gaps on both sides (**Fig. 7**). It supports the thermochemical material and also provides air flow path. The gap is at 4 mm. The reactor is divided into 4 containers. Each container supports 5 kg zeolite 13X. Pipes with diameter at 16 mm are distributed across the containers where the water can flow through the containers. To enhance the heat transfer, copper fins have been integrated in the reactor. Each pipe is attached with 19 fins. The distance between any two fins is 25 mm (details given in Table 2). To measure the temperature of a container, 6 thermocouples are installed in each container. Water temperature is measured by thermocouples located at the inlet and outlet water of a container.

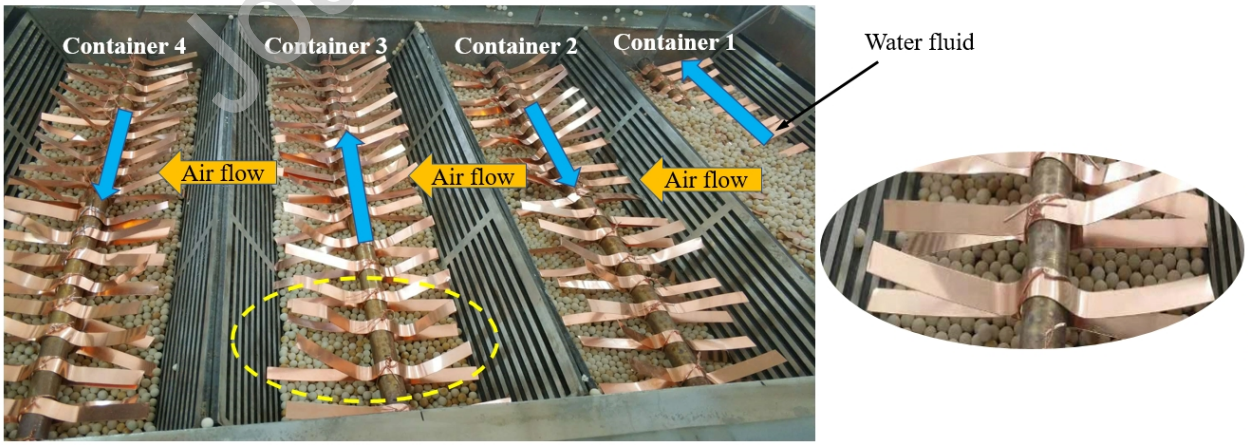

Fig. 7. Picture of the attached copper fins reactor

Table 2

Properties of the zeolite 13X, characteristics of smooth pipe, fins and reactor

Item	Parameters	Value
Zeolite 13X [31]	Bulk density	730 kg/m^3
	Porosity	0.395
	Specific heat capacity	1080 J/kg·K
	Average particle radius	1.15*10^{-3} m
	Thermal conductivity	3.3 W/m·K
Copper fins	Thermal conductivity	386.4 W/m·K
	Number of each pipe	19
	Thickness	0.0003 m
	Length	0.12 m
	Width	0.01 m
	Spacing pitch	0.025 m
Copper pipe	Inner diameter	0.014 m
	Outer diameter	0.016 m
Reactor	Length	1 m
	Width	0.5 m
	Height	0.1 m
	Insulation thickness	0.03 m

3.3. Reactor performance indicator

Thermal power transferred to the reactor in charging and release from the reactor in discharging process can be calculated by Eq.(1) and Eq.(2).

$$\dot{Q}_{\text{char}} = \dot{m}_{\text{char}} \cdot c_{\text{p}} \cdot \left(T_{\text{in}} - T_{\text{out}}\right) \tag{1}$$

$$\dot{Q}_{\text{dis}} = \dot{m}_{\text{dis}} \cdot c_{\text{p}} \cdot \left(T_{\text{out}} - T_{\text{in}}\right) \tag{2}$$

where $\dot{m}$ and c_P refers to the air mass flow rate and specific heat capacity of the air respectively, T_{in} and T_{out} represent for the air inlet and outlet air temperature of reactor. The accumulated thermal energy output and energy input can be expressed by Eq.(3) and Eq.(4).

$$Q_{\text{dis}} = \int_0^{t_{\text{dis}}} \dot{Q}_{\text{dis}} \mathrm{d}t = \dot{m}_{\text{dis}} \cdot c_{\text{p}} \cdot \int_0^{t_{\text{dis}}} \left(T_{\text{out}} - T_{\text{in}}\right) \mathrm{d}t \tag{3}$$

$$Q_{\text{char}} = \int_0^{t_{\text{char}}} \dot{Q}_{\text{char}} \mathrm{d}t = \dot{m}_{\text{char}} \cdot c_{\text{p}} \cdot \int_0^{t_{\text{char}}} \left(T_{\text{in}} - T_{\text{out}}\right) \mathrm{d}t \tag{4}$$

The absolute humidity of air is calculated by using Eq.(5) [32]:

$$\omega = 216.7 \times \left[\frac{\frac{RH}{100\%} \times 6.112 \times \exp\left(\frac{17.62 \times T}{243.12 + T} \right)}{273.15 + T} \right] \quad (5)$$

where RH (the relative humidity) is the ratio of the moisture content of the air to the saturation moisture content at any specific condition.

3.4. Experimental uncertainty analysis

The uncertainty of the experimental test relating to temperature, pressure, flow and relative humidity, is calculated by using Eq.(6) [33].

$$U = \pm \sqrt{\left(\frac{\Delta T_{TC}}{T_{TC}} \right)^2_{reactor} + \left(\frac{\Delta T_{TC}}{T_{TC}} \right)^2_{air} + \left(\frac{\Delta RH}{RH} \right)^2_{air} + \left(\frac{\Delta P}{P} \right)^2_{air} + \left(\frac{\Delta V}{V} \right)^2_{air} + \left(\frac{\Delta V}{V} \right)^2_{water}} \times 100\% \quad (6)$$

According to the instrumentation specifications in Table 1, the overall uncertainty is ± 5.29%.

4. Experiment results and discussions

The experimental tests are conducted according to the flowchart **Fig. 6**. Table 3 gives the experimental operation conditions.

Table 3

Typical operation parameters of experimental test

Operation parameters	Charging test	Discharging test
Inlet air temperature	180 ℃	22-26 ℃
Vapour pressure	460-480 Pa	200-220 Pa
Relatively humidity of the inlet air	0 %	95-99 %
Airflow rate	200-300 kg/h	57 kg/h
Water flow rate	0 m^3/h	0.08 m^3/h
Water temperature	-	25-28 ℃

4.1. Performance of smooth pipe and copper fins reactor in charging

Fig. shows the temperature profile of smooth pipes reactor in a charging test. The temperature of container 1 and 2 increases sharply in 2 hours and reaches to the inlet air temperature after 4 hours. The temperature of container 3 and 4 reach to the peak at 171 ℃ for container 3 and at 168 ℃ for container 4.

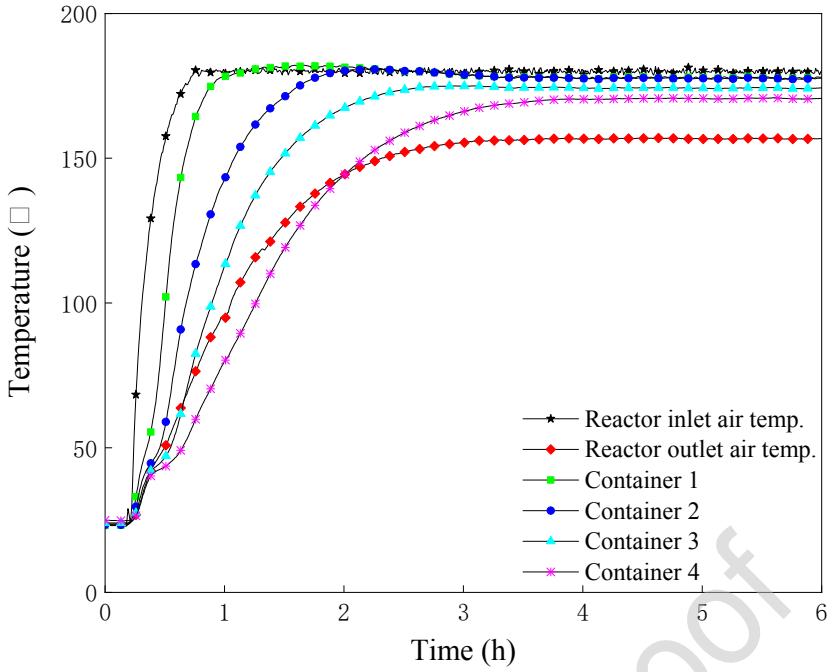

Fig. 8. Reactor temperature profile for case 1 in the charging test

Fig. depicts the reactor pressure drop and air flow rate during the charging test. The air pressure ranges from 460 Pa to 480 Pa and air flow rate varies fluctuates at around 200 kg/h to 300 kg/h.

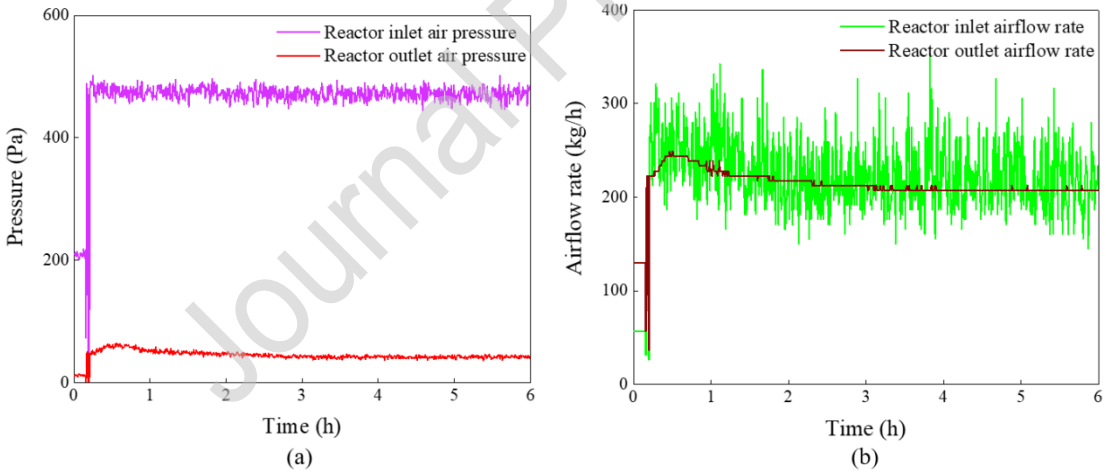

Fig. 9. (a) Air pressure drop and (b) airflow rate for case 1 in the charging

Comparisons have been given for smooth pipes and copper fins reactor. Fig. 10 depicts absolute humidity of air at inlet and outlet of the reactor in a charging process. For both cases, the absolute humidity drops along with charging process. However, the smooth pipe reactor (case 1) requires relatively longer time for it reducing to the level of copper fins reactor (case 2). For the difference of absolute humidity at the reactor inlet and outlet, as shown in **Fig.** (b), the smooth pipe reactor (case 1) and copper fins reactor (case 2) takes 1.16 hours and 0.62 hours to reach close to zero, respectively. It indicates that copper fins have accelerated the charging process by enhancing heat transfer within the reactor.

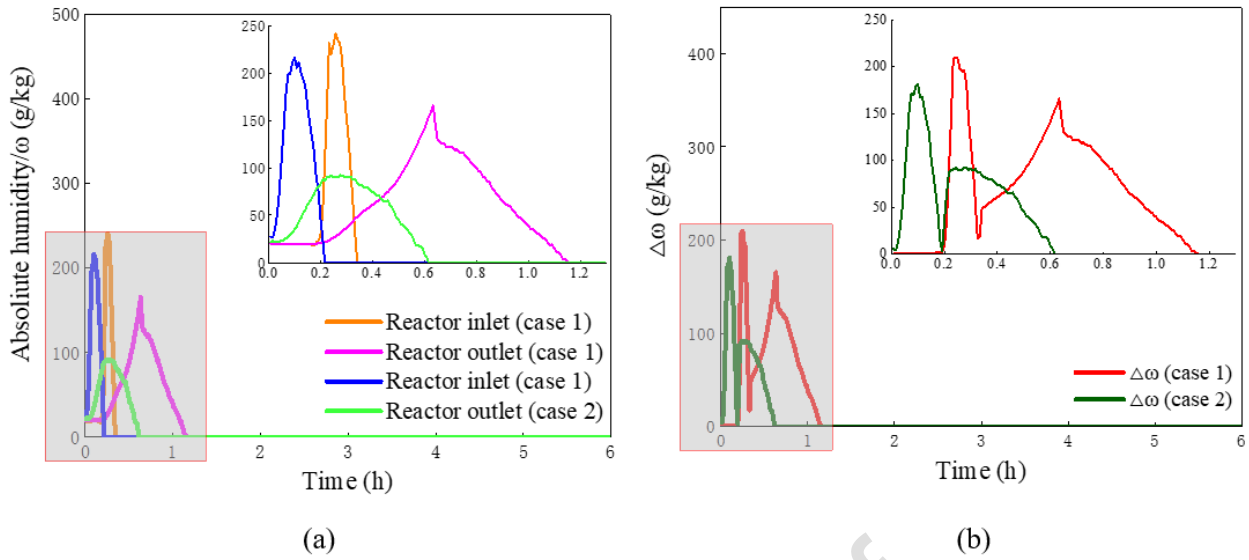

Fig. 10. (a) Absolute humidity of air flow for smooth pipe and copper fins reactor in charging, (b) change of the absolute humidity for the two cases

The enhancement in heat transfer can also be reflected from the reactor inlet and outlet air temperature. **Fig.** shows the reactor inlet and outlet air temperature difference for both cases. The case 1 reaches the peak temperature difference at 114 ℃ in 0.55 hours and case 2 peaks at 84.68 ℃ in 0.28 hours. This shows that the zeolite in copper fins reactor has achieved relatively higher temperature in reduced time, therefore achieving a lower temperature difference between the inlet and outlet air.

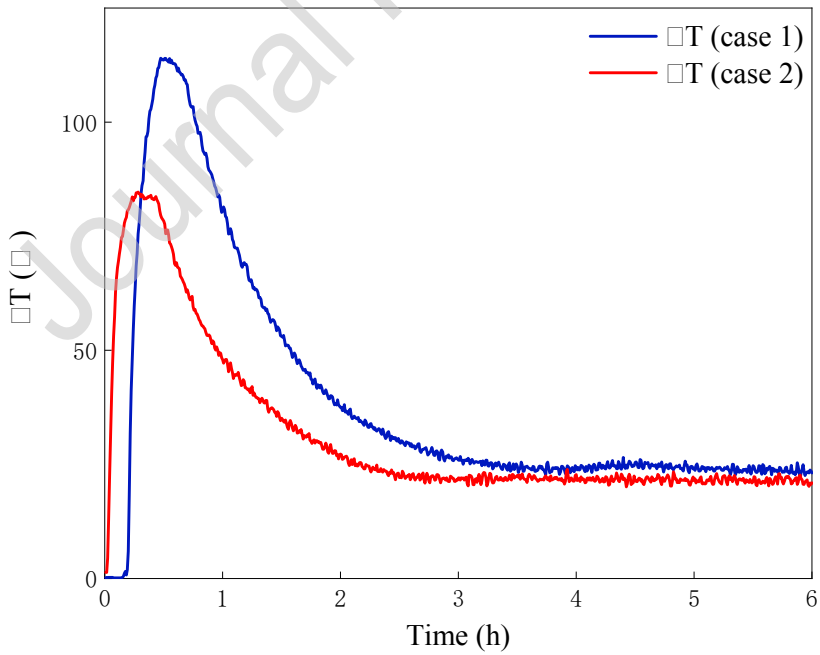

Fig. 11. Reactor inlet and outlet air temperature difference for case 1 and case 2

In addition to the inlet and outlet air temperature and humidity, Table 4 shows the container's peak temperature and the corresponding achieving duration in the charging processes. Case 2 achieves relatively higher peak temperature than that of the case 1 in less time. For the outlet air temperature,

copper fins reactor achieves the peak outlet air temperature at 158.7 ℃ in 2.88 hours. While it takes 3.63 hours for smooth pipes reactor to reach the peak at 156.2 ℃. Overall, the tests have shown that the integration of copper fins lifts the reactor charging performance.

Table 4

Peak temperature of containers and the achieving duration for case 1 and case 2

Case	Container 1		Container 2		Container 3		Container 4		Reactor outlet air temperature (ºC)	
	Peak temperature (ºC)	Time (h)	Peak temperature (ºC)	Time (h)	Peak temperature (ºC)	Time (h)	Peak temperature (ºC)	Time (h)	Peak temperature (ºC)	Time (h)
1	178	1	175	1.9	171	3.26	168	3.8	156.2	3.63
2	180	1.55	180	1.79	177	2.76	174	2.9	158.7	2.88

4.2. Performance of smooth pipes and copper fins reactor in discharging

Discharging tests have been conducted according to the operation conditions in Table 3 for case 1 and case 2. **Fig.** shows the air flow parameters in the tests including relative humidity and pressure.

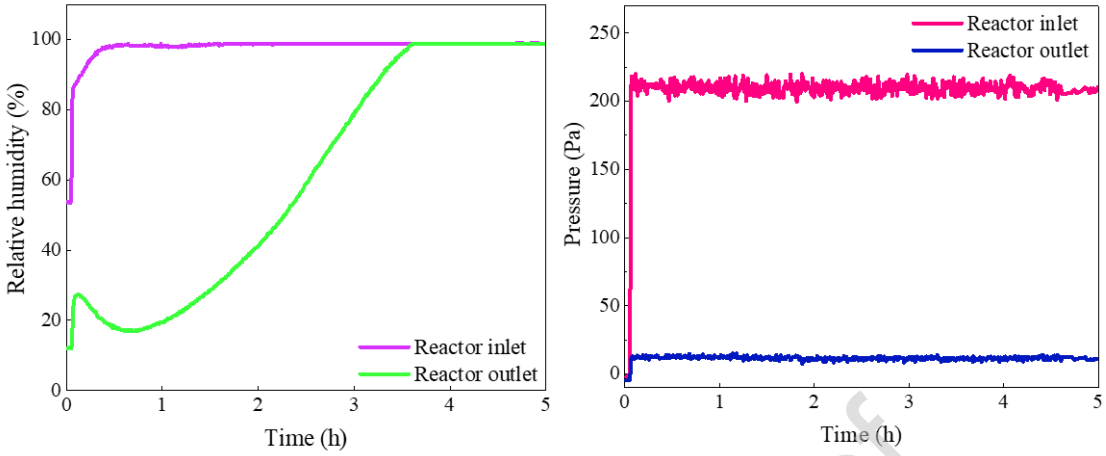

Fig. 12. Air flow parameters in the discharging tests: (a) relative humidity, (b) air pressure drop

Fig. shows the absolute humidity of air in both reactor tests. Due to hygroscopic characteristics of zeolite 13X at the beginning of the discharging, absolute humidity at the reactor outlet for case 1 and case 2 both increases quickly. Obviously, the absolute humidity for case 2 fluctuates from 1.23 hours to 1.69 hours, which indicates the possible unstable operating conditions.

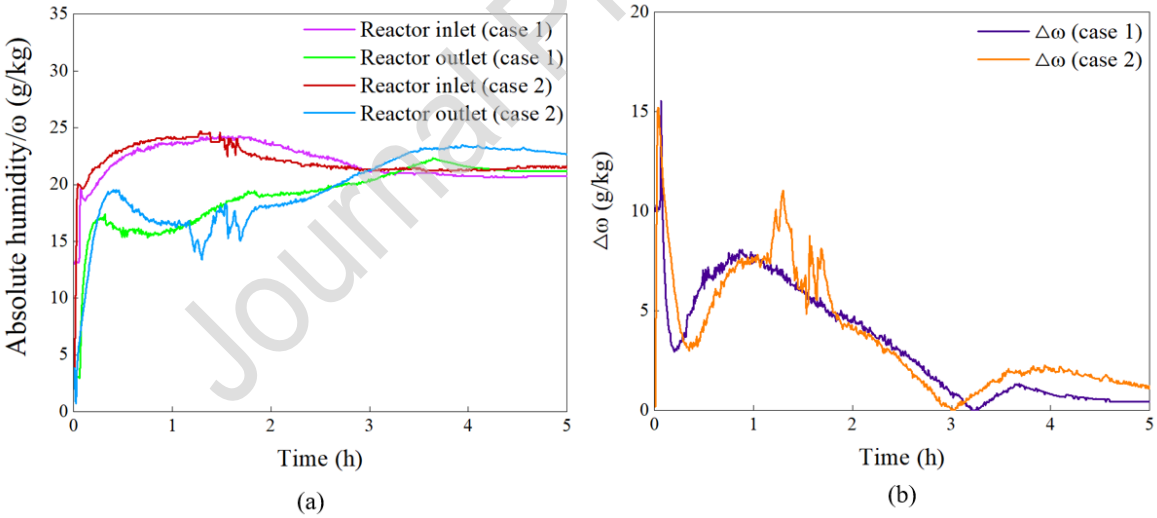

Fig. 13. (a) the absolute humidity of reactor of air and (b) inlet and outlet air absolute humidity difference

When considering water as heat output in discharging, **Fig.** shows the reactor outlet water and reactor outlet air temperature for both cases. Under the same inlet water temperature at 25 ℃, case 2 achieves the higher water temperature at over 35 ℃ and case 1 reaches to around 30 ℃. This shows copper fins boost the heat transfer between the zeolites and water. For the reactor outlet air temperature in the discharging process, both cases show similar temperature trend. However, case 2 achieves 2 ℃ to 5 ℃ higher than that of the case 1.

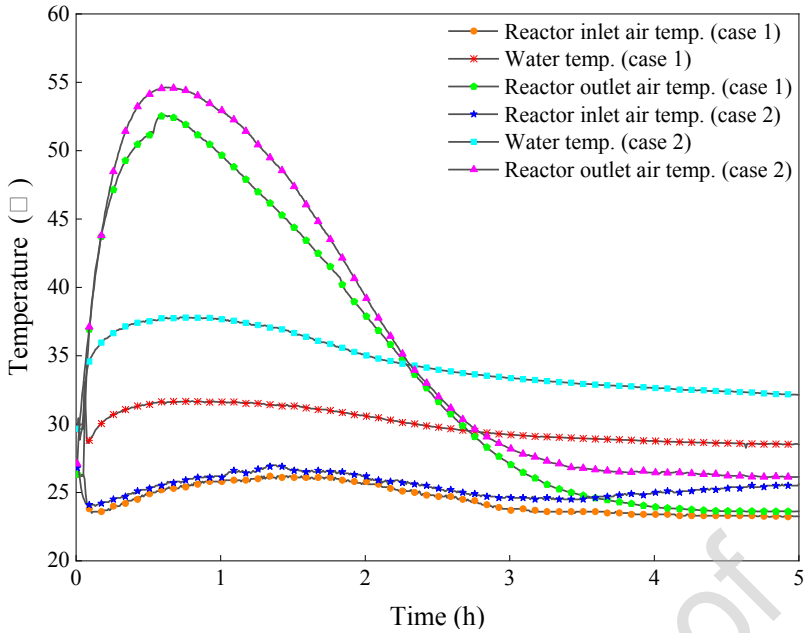

Fig. 14. Air and water temperature in discharging for case 1 and case 2

Table 5 summaries the average reactor container temperature and water temperature lift for case 1 and case 2. Case 2 has shown superior performance than case 1 including the container temperature, reactor outlet air temperature, and reactor outlet water temperature. In terms of water flow, case 2 provides water temperature lift at 9.7 ℃ which is 4 ℃ higher than case 1. For reactor outlet air, case 2 is 2 ℃ higher than that of case 1. For the container temperature, for instance, Container 3 achieves the peak container temperature at 66.2 ℃, 1.4 ℃ higher than that of case 1. The data indicate that copper fins reactor has achieved the improved performance in reaching relatively higher water and outlet air temperature in discharging.

Table 5

Comparison of air and water temperature for case 1 and case 2 in the discharging

Case	Inlet air temperature (℃)	Average reactor temperature (℃)				Outlet air temperature (℃)	Max outlet water temperature (℃)	Water temperature lift (℃)
		Container 1	Container 2	Container 3	Container 4			
	Min-Max	Min-Max	Min-Max	Min-Max	Min-Max	Min-Max		
1	23.6-26.3	23.1-46..2	23.3-60.5	23.9-64.8	24.8-67.7	26.3-52.6	35.4	5.7
2	24-27	24.7-45.1	25.7-59.8	26.4-66.2	27.9-69.8	26.1-54.6	39.4	9.7

4.3. Performance analysis

Power, energy storage density and energy efficiency in the charging and discharging have been calculated and presented in Table 6. The copper fins reactor in case 2 achieves a relatively higher energy efficiency with lower power input required in discharging. For energy density with respect to the volume of thermochemical material and reactor, the smooth pipe reactor achieves 246 kWh/m^3 (material) and 135 kWh/m^3 (reactor); the copper fins reactor achieves 233 kWh/m^3 (material) and 128 kWh/m^3 (reactor).

Table 6

Comparison on the power input, output, energy storage density and efficiency

Case	Average power input (kW)	Average power output (kW)	Energy storage density (kWh/m^3) (material)	Energy storage density (kWh/m^3) (reactor)	Energy efficiency
1	2.36	1.35	246	135	0.48
2	2.02	1.28	233	128	0.53

Table 7 gives comparison analysis of the energy storage density with different prototypes in previous studies. By applying the copper fins, the current study stands out in achieving water temperature lift varying from 5.7 ºC to 9.7 ºC and comparable reactor outlet air temperature in discharging. Additionally, the copper fins have improved the charging performance, enabling the reactor to achieve a relative higher energy density in charging and energy efficiency in charging and discharging cycles.

Table 7

Comparison of key findings of the study with the literature

Study	Year	Thermochemical material	Charging temperature (ºC)	Discharging temperature (ºC)	Key findings
Present study	2019	20 kg zeolite 13X	180	25-30	• Energy density for material is 233 kWh/m^3 and for the copper fins reactor is 128 kWh/m^3 • Reactor outlet air temperature at 55 ℃ • Effective water temperature lift is between 5.7 and 9.7 ℃ • Reactor efficiency of 48-53%
[34]	2008	70 kg zeolite 4A	170	20	• Energy density at 120 kWh/m^3 • Max outlet air temperature of reactor at 42 ºC
[35]	2012	7000 kg zeolite 13X	130	25	• Energy density at 135 kWh/m^3 • Max outlet air temperature of reactor at 100 ºC • A maximum heating power of 95 kW
[7]	2014	50 kg zeolite 4A/X	180-230	25	• Energy density at 148 kWh/m^3 • Reactor outlet air temperature peak at 60 ºC • Generate adsorption heat up to 12 kWh • Temperature shifts of process air up to 36 ºC
[36]	2014	150 kg zeolite 13X	185	25-60	• Energy density at 58 kWh/m^3 • Max outlet air temperature of reactor at 70 ºC
[37]	2015	80 kg zeolite13X	120-180	20	• Energy density at 114 kWh/m^3 • Max outlet air temperature of reactor at 57 ºC • Supply a constant power of 2.25kW
[38]	2016	88.2 L zeolite 13X	80	20	• Energy density ranges from 55 to 85 kWh/m^3 • Outlet air temperature of reactor ranges from 31.9 to 59.6 ºC

[6]	2018	250 L zeolite 13X	180	10-55	• Energy density ranges from 81 to 136 kWh/m^3 • Max outlet air temperature of reactor at 75 ºC

5. Conclusions

This paper experimentally investigates a copper fins thermochemical reactor for building's applications. To enhance the heat transfer performance, copper fins have been integrated into the reactor. The charging and discharging performance of the reactor have been evaluated and compared with the reactor without fins. Key findings of the study are listed as follow.

- Copper fins reactor achieves faster temperature increase in charging due to the heat transfer enhancement. It takes 2.88 hours for copper fins reactor reaching the outlet air temperature at 158.7 ºC. However, for the reactor without fins, it takes 3.63 hours to reach at 156.2 ℃. The copper fins reactor achieves better charging performance and reduce the energy consumption in charging.
- In discharging, comparing to the smooth pipe reactor, the copper fins reactor achieves higher temperature output in both outlet air and outlet water. According to the experimental tests, for the outlet air temperature, the copper fins reactor achieves the peak value at 54.6 ℃, 2 ℃ higher than that of the smooth pipes reactor. For the water outlet temperature, copper fins reactor reaches to the peak at 39.4 ℃, 4 ℃ higher than that of the smooth pipes reactor.
- According to the experimental tests, energy density of copper fins reactor is comparable to the previous study with 233 kWh/m^3 for material level and for 128 kWh/m^3 for the reactor level. Additionally, energy efficiency of copper fins reactor reaches to 53% in contrast to the smooth pipes reactor at 48%.
- In addition to the reactor design, operational parameters can affect the reactor performance including the humidity, air flowrate, inlet air temperature, etc. Further studies are required to improve the reactor performance with better controls in the parameters.
- Thermal losses to the ambient is an issue in charging and discharging cycles which shall be tackled to improve the energy efficiency.

Reference

[1] D. Aydin, S.P. Casey, and S. Riffat, The latest advancements on thermochemical heat storage systems. Renewable and Sustainable Energy Reviews. 41 (2015) 356-367.

[2] T.X. Li, S. Wu, T. Yan, R.Z. Wang, et al., Experimental investigation on a dual-mode thermochemical sorption energy storage system. Energy. 140 (2017) 383-394.

[3] P. Tatsidjodoung, N. Le Pierrès, J. Heintz, D. Lagre, et al., Experimental and numerical investigations of a zeolite 13X/water reactor for solar heat storage in buildings. Energy Conversion and Management. 108 (2016) 488-500.

[4] M.Gaeini, M.R.Javed, H.Ouwerkerk, H.A.Zondag, et al., Realization of a 4kW thermochemical segmented reactor in household scale for seasonal heat storage. 11th International Renewable Energy Storage Conference,IRES 2017. 135 (2017) 105-114.

[5] M. Gaeini, R. van Alebeek, L. Scapino, H.A. Zondag, et al., Hot tap water production by a 4 kW sorption segmented reactor in household scale for seasonal heat storage. Journal of Energy Storage. 17 (2018) 118-128.

[6] R. van Alebeek, L. Scapino, M.A.J.M. Beving, M. Gaeini, et al., Investigation of a household-scale open sorption energy storage system based on the zeolite 13X/water reacting pair. Applied Thermal Engineering. 139 (2018) 325-333.

[7] B. Zettl, G. Englmair, and G. Steinmaurer, Development of a revolving drum reactor for open-sorption heat storage processes. Applied Thermal Engineering. 70(1) (2014) 42-49.

[8] C. Finck, E. Henquet, C. van Soest, H. Oversloot, et al., Experimental Results of a 3 kWh Thermochemical Heat Storage Module for Space Heating Application. Energy Procedia. 48 (2014) 320-326.

[9] R. Cuypers, N. Maraz, J. Eversdijk, C. Finck, et al., Development of a Seasonal Thermochemical Storage System. Energy Procedia. 30 (2012) 207-214.

[10] C. Bales, Thermal properties of materials for thermo-chemical storage of solar heat, development. 20 (2005).

[11] K.C. Leong and Y. Liu, Numerical modeling of combined heat and mass transfer in the adsorbent bed of a zeolite/water cooling system. Applied Thermal Engineering. 24(16) (2004) 2359-2374.

[12] S. Pal, M.R. Hajj, W.P. Wong, and I.K. Puri, Thermal energy storage in porous materials with adsorption and desorption of moisture. International Journal of Heat and Mass Transfer. 69 (2014) 285-292.

[13] R. Sizmann, D. Jung, and N. Khelifa, Storage of low temperature heat by thermochemical reactions. Cooperation Meditterraneenne Pour Lenergie Solaire. (1981) 42-51.

[14] R. Gopal, B.R. Hollebone, and C.H. Langford, The rates of solar energy storage and retrieval in a zeolite-water system. Solar Energy. 28(5) (1982) 421-424.

[15] B. Mette, H. Kerskes, and H. Drück, Experimental and Numerical Investigations of Different Reactor Concepts for Thermochemical Energy Storage. Energy Procedia. 57 (2014) 2380-2389.

[16] J. Jänchen, D. Ackermann, H. Stach, and W. Brösicke, Studies of the water adsorption on Zeolites and modified mesoporous materials for seasonal storage of solar heat. Solar Energy. 76(1-3) (2004) 339-344.

[17] H. Bjurström, E. Karawacki, and B. Carlsson, Thermal conductivity of a microporous particulate medium: moist silica gel. Int. J. Heat Mass Transf. 27 (1984) 2025-2036.

[18] A. Solé, X. Fontanet, C. Barreneche, I. Martorell, et al., Parameters to take into account when

developing a new thermochemical energy storage system. Energy Procedia. 30 (2012) 380-387.
[19] G.T. Whiting, D. Grondin, D. Stosic, S. Bennici, et al., Zeolite–$MgCl_2$ composites as potential long-term heat storage materials: Influence of zeolite properties on heats of water sorption. Solar Energy Materials and Solar Cells. 128 (2014) 289-295.
[20] M. Richter, M. Bouché, and M. Linder, Heat transformation based on $CaCl_2$ /H_2O – Part A: Closed operation principle. Applied Thermal Engineering. 102 (2016) 615-621.
[21] A. Fopah Lele, F. Kuznik, O. Opel, and W.K.L. Ruck, Performance analysis of a thermochemical based heat storage as an addition to cogeneration systems. Energy Conversion and Management. 106 (2015) 1327-1344.
[22] A.-J. de Jong, F. Trausel, C. Finck, L. van Vliet, et al., Thermochemical Heat Storage – System Design Issues. Energy Procedia. 48 (2014) 309-319.
[23] C.J. Ferchaud, Experimental study of salt hydrates for thermochemical seasonal heat storage door. No. (April，2016).
[24] L. Scapino, H.A. Zondag, J. Van Bael, J. Diriken, et al., Sorption heat storage for long-term low-temperature applications: A review on the advancements at material and prototype scale. Applied Energy. 190 (2017) 920-948.
[25] B. Michel, N. Mazet, and P. Neveu, Experimental investigation of an innovative thermochemical process operating with a hydrate salt and moist air for thermal storage of solar energy: Global performance. Applied Energy. 129 (2014) 177-186.
[26] F. Trausel, A.-J. de Jong, and R. Cuypers, A Review on the Properties of Salt Hydrates for Thermochemical Storage. Energy Procedia. 48 (2014) 447-452.
[27] K. G and S. D, The chemistry and electrochemistry of magnesium production. Adv Molten Salt Chem. 6 (1987) 127-209.
[28] P.A.J. Donkers, L.C. Sögütoglu, H.P. Huinink, H.R. Fischer, et al., A review of salt hydrates for seasonal heat storage in domestic applications. Applied Energy. 199 (2017) 45-68.
[29] E.-P. Ng and S. Mintova, Nanoporous materials with enhanced hydrophilicity and high water sorption capacity. Microporous and Mesoporous Materials. 114(1-3) (2008) 1-26.
[30] L.W. Wang, R.Z. Wang, and R.G. Oliveira, A review on adsorption working pairs for refrigeration. Renewable and Sustainable Energy Reviews. 13(3) (2009) 518-534.
[31] H. O.Helaly, M. M.Awad, E.-S. Ibrahim I, and A. M.Hamed, Theoretical and experimental investigation of the performance of adsorption heat storage system Applied Thermal Engineering. 147 (2019) 10-28.
[32] D. Aydin, S.P. Casey, X. Chen, and S. Riffat, Numerical and experimental analysis of a novel heat pump driven sorption storage heater. Applied Energy. 211 (2018) 954-974.
[33] D.Zhou and C.Y.Zhao, Experimental investigations on heat transfer in phase change materials (PCMs) embedded in porous materials. Applied Thermal Engineering. 31 (2011) 970-977.
[34] C. Bales, P. Gantenbein, D. Jaenig, H. Kerskes, et al., Laboratory tests of chemical reactions and prototype sorption storage units. A Report of IEA Solar Heating and Cooling programme-Task 32.
[35] A.H. Abedin and M.A. Rosen, Closed and open thermochemical energy storage: Energy- and exergy-based comparisons. Energy. 41(1) (2012) 83-92.
[36] S.S. R. de Boer, H.A. Zondag, G. Krol, Development of a prototype system for seasonal solar heat storage using an open sorption process. (2014) 28-30.
[37] K. Johannes, F. Kuznik, J.-L. Hubert, F. Durier, et al., Design and characterisation of a high

powered energy dense zeolite thermal energy storage system for buildings. Applied Energy. 159 (2015) 80-86.

[38] D. Aydin, S.P. Casey, X. Chen, and S. Riffat, Novel "open-sorption pipe" reactor for solar thermal energy storage. Energy Conversion and Management. 121 (2016) 321-334.

Declaration of interest

The authors declare that they have no known competing financial interests or personal relationships that could have appeared to influence the work reported in this paper.

Highlights

- This paper presents an experimental study of a copper fins thermochemical reactor.
- Copper fins pipe is integrated with the reactor to enhance the reactor performance.
- Experimental tests of charging and discharging have been conducted and presented.
- The reactor achieves peak outlet air temperature at 54.6 ℃ and peak outlet water temperature at 39.4 ℃.
- The reactor achieves energy storage density at 233 kWh/m^3 for material level and 128 kWh/m^3 for the reactor level.